

Date of publication xxxx 00, 0000, date of current version xxxx 00, 0000.

Digital Object Identifier 10.1109/ACCESS.2017.Doi Number

Anti-shadowing Resource Allocation for General Mobile Cognitive Radio Networks

Miao Liu¹, (IEEE Student Member), Tiecheng Song¹, (IEEE Member), Jing Hu¹, (IEEE Member), Hikmet Sari², (IEEE Fellow), and Guan Gui², (IEEE Senior Member)

¹National Mobile Communications Research Laboratory, Southeast University, Nanjing, China

²College of Telecommunication and Information Engineering, Nanjing University of Posts and Telecommunications, Nanjing, China.

Corresponding author: Tiecheng Song (e-mail: songtc@seu.edu.cn).

This work was supported by the National Natural Science Foundation of China under Grant No. 61372104 and No. 61271207.

ABSTRACT Resource allocation (RA) for mobile secondary users (SUs) is considered one of the most important techniques for designing the next-generation cognitive radio network (CRN). In this paper, ‘effective capacity (EC)’ is proposed to improve the RA performance for an underlay-based mobile CRN. By optimizing EC, an efficient resource allocation scheme is developed. First, we consider a moving secondary system where the channel state information (CSI) can be predicted by location-awareness techniques. According to the prediction result, we set protecting parameters for both the secondary and the primary performance targets to minimize the prediction error introduced by the decorrelated shadowing. Second, the computed sum average EC of the cognitive system is maximized. To solve the optimization RA problem, a low-complexity stepwise algorithm is proposed based on four procedures aimed at access, initialization, subchannel and power. Moreover, the speeds of the primary users (PUs) are taken into account, and a general system model is built. The corresponding resource allocation solutions can be induced easily through extending the originally proposed solution. Finally, simulation results are provided to confirm the EC based algorithm. The proposed approach can not only improve the total secondary capacity but also achieve higher energy efficiency (EE) and spectrum efficiency (SE) for the mobile secondary system.

INDEX TERMS Anti-shadowing, CSI predicting, effective capacity, mobile cognitive radio network, resource allocation.

I. INTRODUCTION

Cognitive radio is considered one of the effective techniques to enhance spectrum utilization [1] in modern and future wireless communication systems. In addition, the orthogonal frequency division multiple access (OFDMA) technique is a domain multiple access strategy that can allocate radio resource flexibility to multiple users [2]. Motivated by the two techniques, secondary users (SUs) in OFDMA-based cognitive radio networks (CRNs) can flexibly share the accessible licensed spectrum with primary users (PUs) if they do not introduce harmful interferences for PUs. Because of their fantastical merits, OFDMA-CRNs have been studied intensely in the past decade. However, there still exist many performance optimization problems in deploying CRNs [3]. For example, the secondary transmission often causes excessive interference to PUs. In addition, the throughput of CRN links may not be optimized for reliable high-quality communications. Furthermore, CRN links lack robustness for mobile SUs. Hence, all of the optimization problems must be solved simultaneously.

It is well known that spectrum sensing [4] can solve the above problems. In previous works, SUs are assumed to be static. Hence, the instantaneous channel state information (CSI) sensed dominates the decisions of the spectrum scheduling and power allocation. However, the static assumption does not hold in mobile CRNs because of the time-variant channel. Hence, the instant sensing results are not able to guide the resource allocation (RA) independently. Moreover, when the SU is moving, the relevance of the shadow fading it suffers on the path becomes lower. This will lead to an enormous difficulty in the analysis of the channel during a continuous time slot. Therefore, the traditional sensing method and access control schemes cannot be directly applied in mobile CRNs.

In recent years, a number of spectrum access schemes in the mobile CRNs have been studied, such as the location-awareness-based power control for concurrent transmissions [5], interweave-based opportunistic spectrum access [6], and trusted collaboration-based spectrum sensing [7]. However, previous works do not consider the channel prediction and

RA problem. Unlike previous works, this paper studies the problem of enabling anti-shadowing channel prediction and RA schemes for general mobile CRNs. First, we present a mobility model for SUs in an OFDMA-based cellular CRN. Different from the model considering SUs' mobility randomly in [6], the proposed model is general and representative because the Mobility State Information (MSI) of SUs is defined and can be predicted through a location-aware spectrum sensing method in our work. This assumption of employing advanced technologies of localization and dynamic sensing is considered reasonable, since the related works are abundant and effective in recent years, especially with the help of wireless sensors [8] - [10]. Next, the anti-shadowing CSI predicting strategy is proposed; this strategy depends on the RA results of the mobile SUs. The specific significance of the CSI in mobile CRNs has also been noticed in a sensing technology-related study for cognitive ad hoc networks [11]. Utilizing the anti-shadowing CSI predicting method, a novel RA scheme is studied. Further, to solve the secondary RA problem in more practical and general scenes, we took the mobility of the PUs into consideration. By extending the basic analyses for static primary networks, a similar RA method can be obtained easily.

The original RA algorithm proposed for the static PUs will be mainly discussed in this paper, with the general case omitted after the key derivations are given. In detail, the RA scheme is a stepwise process, and several sub-algorithms are employed to manage the secondary radio resources. It improves both the energy efficiency (EE) and the spectrum efficiency (SE) of the mobile SUs at the same time while maximizing the sum effective capacity (EC) of the secondary network and compensating for the performance loss caused by shadow fading. Promoting EE and SE in wireless communications has become essential and attracted increasing focus from industrial and academic fields [12]. In addition, EC reflects the location-related and time-varying characteristics of the mobile transmission in secondary systems. As a result, evaluation of the EE and the SE of CRNs with effective power (EP) and effective subchannels (ES) is proposed. To the best of our knowledge, there are no prior works studying the general mobility, anti-shadowing CSI prediction, corresponding RA scheme and the impact on EE and SE for the mobile CRNs.

The major contributions of this paper are summarized as follows:

We propose building a CRN model based on the MSI of mobile SUs. Our model takes into consideration both the speed and the direction of SUs, and using this model allows decisive analysis of the access and transmission of SUs.

We study an innovative method involving the use of spectrum sensing results to predict the CSI and transmission performance of SUs when particular subchannels and certain power levels are assigned. To compensate for the performance loss resulting from the prediction error, a protecting parameter is discussed to overcome the location-dependent shadow fading.

A resource allocation scheme based on effective capacity is designed. Through optimization, a low-complexity stepwise algorithm is proposed based on a modification of the algorithm of reference [13]. According to simulations and comparisons, we find that our scheme outperforms the existing schemes in terms of improving the sum effective capacity, the SE and EE of the SUs.

To allow our work to be of more practical value and extensive significance, a general system model is interdependently discussed. The mobility of both PUs and SUs is considered at the same time. The key formulas are obtained, and the corresponding RA scheme can be derived in a similar manner.

The rest of this paper is organized as follows. The system model based on mobile SUs is introduced in Section II. Section III discusses the anti-shadowing CSI predicting strategy, followed by the formulated optimization problem and the corresponding algorithm in Section IV and Section V, respectively. In addition, the general scene related to mobile PUs is also discussed at the end of Section V. Simulation results are illustrated and commented on in Section VI. Finally, this work is concluded in Sections VII.

II. SYSTEM MODEL

We consider the RA problem for the secondary downlink in an OFDMA-based CRN, which consists of M pairs of static peer-to-peer (P2P) PUs and N mobile cellular SUs. The paired PUs represent a general form of the ad hoc and the cellular networks. In addition, the centralized secondary network is able to guarantee the communication connectivity and quality of the moving secondary users. In actual situations, the mobile secondary system can be the V2I or V2R communications in the internet of vehicle (IoV) [1]. If the PUs' information is assumed unavailable to the secondary system, the mobility of the PUs is ignored.

In detail, the system comprises a secondary base station (SBS), communicating with the secondary users SU_j ($j = 1, \dots, N$) passing through. The PUs settled under the coverage of the SBS are depicted in Fig. 1(a). As illustrated, PUT_i and PUR_i denote the transmitter and the receiver, respectively, of the i th pair of PUs ($i = 1, \dots, M$). In addition, since the SUs are mobile, we take $SU_j(t_0)$ as the state of SU_j at an earlier time point t_0 and $SU_j(t_1)$ as the state at a later time point t_1 in Fig. 1(a).

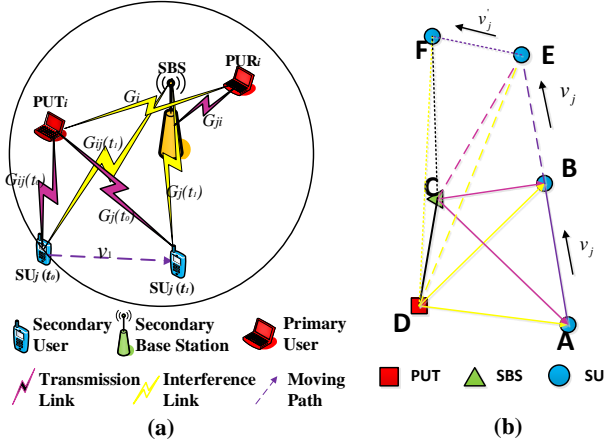


Figure 1. Mobile CRN system model.

The available licensed spectrum is assumed to be divided into Z subchannels of equal bandwidth B_0 . For convenience, we define \mathbf{n}_i to represent the set of pair PU_i 's subchannels. Moreover, $G_{i,z}^P$ is the power gain from PUT_i to PUR_i . Similarly, $G_{j,z}^S(t_0)$ and $G_{j,z}^S(t_1)$ are the gains from SBS to $SU_j(t_0)$ and $SU_j(t_1)$, respectively, on subchannel z . $g_{z,j}^S$, $g_{z,j}^S(t_0)$ and $g_{z,j}^S(t_1)$ denote the interference gains of the link SBS- PUR_i and PUT_i - SU_j on subchannel z . Specifically, v_j represents the speed of SU_j , and N_0 is the noise power spectral density. In this system, techniques for location-awareness and channel estimation are assumed to be applied. As a result, the secondary network is considered to have a perfect knowledge of the location information and the instantaneous CSI.

In the temporal and spatial domains, the system model can be simplified as in Fig. 1(b). As SU_j moves from location A to location B at a constant speed of v_j during time slot $[t_0, t_1]$, the instantaneous channel gains and interference on links CA, DA, CB and DB can be sensed. In detail, the gain between SBS and SU_j on subchannel z and the interference power from the corresponding PU can be expressed as follows:

$$G_{j,z}^S(t_0) = G_{CA}^S = PL_{CA} H_z(t_0), \quad (1)$$

$$G_{j,z}^S(t_1) = G_{CB}^S = PL_{CB} H_z(t_1), \quad (2)$$

$$\begin{aligned} I_{z,j}^P(t_0) &= g_{z,j}^P(t_0) P_z^P + N_0 B_0 \\ &= I_{DA}^P = PL_{DA} H_z(t_0) P_z^P + N_0 B_0, \end{aligned} \quad (3)$$

$$\begin{aligned} I_{z,j}^P(t_1) &= g_{z,j}^P(t_1) P_z^P + N_0 B_0 \\ &= I_{DB}^P = PL_{DB} H_z(t_1) P_z^P + N_0 B_0, \end{aligned} \quad (4)$$

where PL_{XY} represents the path loss gain between locations X and Y and $H_z(t)$ is the multipath fading gain on the subchannel z at the time point t . Because the OFDMA scheme is also applied in primary system, we take P_z^P as the power for PUT_i on subchannel z , if it belongs to the i th pair of PUs. It is reasonable to consider that the time durations of the spectrum sensing and transmitting are very short; thus, the multipath channels can be characterized as slow fading,

i.e., $H_z(t_0) = H_z(t_1) \equiv H_z$.

Further, considering the approximate path loss models such as the Okumara model, we can rewrite the PL_{XY} gain in decibels as

$$PL_{CA}[\text{dB}] = PL_{CA}(h, f) - F(h) \lg d_{CA} + x_{\sigma}^{CA}(t_0), \quad (5)$$

$$PL_{CB}[\text{dB}] = PL_{CB}(h, f) - F(h) \lg d_{BC} + x_{\sigma}^{CB}(t_1), \quad (6)$$

where $PL_{XY}(h, f)$ denotes the part of path loss related to the height of SU's antenna h and the transmitting frequency f . $F(h)$ is a function related to the antenna height of the SU. x_{σ}^{XY} represents the shadow fading gain between locations X and Y and follows a time-varying normal distribution:

$$x_{\sigma}^{XY}(t) \sim N(0, \sigma_{XY}^2), \quad (7)$$

where the standard deviation σ_{XY} is usually taken from 4 dB to 13 dB. If all SUs' antenna heights are assumed equal and the transmitting frequencies are definitely fixed during a transmission slot, then the path loss can be simplified as

$$PL_{CA}[\text{dB}] = K - 10\alpha \lg d_{CA} + x_{\sigma}^{CA}(t_0), \quad (8)$$

$$PL_{CB}[\text{dB}] = K - 10\alpha \lg d_{BC} + x_{\sigma}^{CB}(t_1), \quad (9)$$

where K denotes a constant and α is the path loss factor.

Considering the speed limitation and road deployment in general traffic scenes, the SUs can be assumed to maintain the current direction and speed for a period of time, if the time interval $\Delta t = t_1 - t_0$ is short enough. Therefore, as is shown in Fig. 1(b), SU_j most likely moves to location E at t_2 . Similarly, $G_{j,z}^S(t_2)$ and $g_{z,j}^S(t_2)$ can be utilized to denote the channel gain for the links CE and DE on subchannel z . Therefore, the CSI for SU_j on subchannel z at t_2 can be expressed as

$$G_{j,z}^S(t_2) = G_{CE}^S = PL_{CE} H_z, \quad (10)$$

$$\begin{aligned} I_{z,j}^P(t_2) &= g_{z,j}^P(t_2) P_z^P + N_0 B_0 \\ &= I_{DE}^P = PL_{DE} H_z P_z^P + N_0 B_0, \end{aligned} \quad (11)$$

III. ANTI-SHADOWING CSI PREDICTING

Combining Eq. (1) to Eq. (11), the relationship between $G_{j,z}^S$ at t_1 and t_2 can be given by

$$\begin{aligned} \frac{G_{j,z}^S(t_2)}{G_{j,z}^S(t_1)} &= 10^{\frac{1}{10}(PL_{CE}[\text{dB}] - PL_{CB}[\text{dB}])} \frac{H_z(t_2)}{H_z(t_1)} \\ &= \left(\frac{d_{CB}}{d_{CE}} \right)^{\alpha} 10^{\frac{1}{10}(x_{\sigma}^{CE}(t_2) - x_{\sigma}^{CB}(t_1))} \end{aligned} \quad (12)$$

The shadow fading in mobile radio systems is known as distance-correlated [A]. When SUs move at high speeds, the instantaneous channel gains change rapidly, and the mutual correlations will be quite low. This indicates that the CSI of SUs might become independent during a transmission time slot and is difficult to predict. Furthermore, the CSI prediction error result from the decorrelated shadowing will cause a series of performance losses.

To compensate for the performance loss, we define the

predictive value for $G_{j,z}^S$ at t_2 with the product of its expectation value multiplied by an error correction coefficient SL . As is known, the correlation coefficient of the shadow fading is related to the speed, transmission time, and decorrelation distance. Moreover, it has been proved that the actual decorrelation distances in various circumstances (such as dense urban, urban, suburban, rural area and high-speed railway) could be easily measured. As a result, SL can be fixed as a constant by presetting the appropriate radius of the CRN and allowed speeds of the SUs.

Because the MSI of SU_j at t_2 (i.e., d_{CE} and d_{DE}) is known, we obtain the following prediction equation:

$$\begin{aligned} G_{j,z}^{S*}(t_2) &= SL \cdot \mathbf{E}[G_{j,z}^S(t_2)] \\ &= SL \cdot \left(\frac{d_{BC}}{d_{CE}}\right)^\alpha \cdot G_{CB}^S \cdot 10^{\frac{1}{10} \mathbf{E}[x_\sigma^{CE} - x_\sigma^{BC}]} \\ &= SL \cdot \left(\frac{d_{BC}}{d_{CE}}\right)^\alpha G_{j,z}^S(t_1), \end{aligned} \quad (13)$$

where $0 < SL < 1$. Similarly, for predicting the interference, $1/SL$ should be multiplied to compensate the prediction loss, aiming to provide more protection to the users' quality of service (QoS). In detail, if the noise power is negligible compared with the accompanied interference, (14) can be deduced as follows:

$$\begin{aligned} I_{z,j}^{P*}(t_2) &= \frac{1}{SL} \cdot \mathbf{E}[I_{z,j}^P(t_2)] \\ &\approx \frac{1}{SL} \cdot \left(\frac{d_{DB}}{d_{DE}}\right)^\alpha I_{DB}^P \cdot 10^{\frac{1}{10} \mathbf{E}[x_\sigma^{DE} - x_\sigma^{DB}]} \\ &= \frac{1}{SL} \cdot \left(\frac{d_{DB}}{d_{DE}}\right)^\alpha I_{z,j}^P(t_1). \end{aligned} \quad (14)$$

Based on location-awareness techniques, the information referring to distance, direction, speed and time composes the set of MSI. With the known information, according to the Cosine Theorem, the MSI at t_2 can be predicted as

$$d_{CE} = \sqrt{d_{CA}^2 + (d_{BA} + v_j(t_2 - t_1))^2 - 2d_{CA}(d_{BA} + v_j(t_2 - t_1))\cos \angle CAB}, \quad (15)$$

$$d_{DE} = \sqrt{d_{DA}^2 + (d_{BA} + v_j(t_2 - t_1))^2 - 2d_{DA}(d_{BA} + v_j(t_2 - t_1))\cos \angle DAB} \quad (16)$$

As the MSI of d_{CA} , d_{DA} , d_{BA} , $\angle CAB$ and $\angle DAB$ are achievable, Eqs. (15)- (16) can be defined as

$$d_{CE} \stackrel{\text{def}}{=} F_d^j(v_j, t_{21}), \quad (17)$$

$$d_{DE} \stackrel{\text{def}}{=} F_d^{i,j}(v_j, t_{21}), \quad (18)$$

where $t_{21} = t_2 - t_1$. Therefore, the CSI at t_2 can be predicted with MSI prediction and spectrum sensing technologies as follows:

$$G_{j,z}^{S*}(t_2) = SL \cdot \left(\frac{d_{CB}}{F_d^j(v_j, t_{21})}\right)^\alpha G_{j,z}^S(t_1), \quad (19)$$

$$I_{z,j}^{P*}(t_2) = \frac{1}{SL} \cdot \left(\frac{d_{DB}}{F_d^{i,j}(v_j, t_{21})}\right)^\alpha I_{z,j}^P(t_1). \quad (20)$$

Thus, the Shannon capacity of SU_j on subchannel z at t_2 is given by

$$\begin{aligned} C_{j,z}^{S*}(t_2) &\approx B_0 \log_2 \left(1 + \frac{G_{j,z}^{S*}(t_2) P_{j,z}^S}{I_{z,j}^{P*}(t_2)} \right) \\ &= B_0 \log_2 \left(1 + SL^2 \cdot \frac{\left(\frac{d_{CB}}{F_d^j(v_j, t_{21})}\right)^\alpha G_{CB}^S P_{j,z}^S}{\left(\frac{d_{DB}}{F_d^{i,j}(v_j, t_{21})}\right)^\alpha I_{DB}^P} \right) \\ &= B \log_2 \left(1 + SL^2 \cdot \frac{P_{j,z}^S G_{j,z}^S(t_1) d_j^\alpha(t_1)}{I_{z,j}^P(t_1) \cdot d_{j,i}^\alpha(t_1)} \cdot \left(\frac{F_d^{i,j}(v_j, t_{21})}{F_d^j(v_j, t_{21})}\right)^\alpha \right) \end{aligned} \quad (21)$$

where $P_{j,z}^S$ is the transmission power on subchannel z for SU_j .

IV. PROBLEM FORMULATION

The primary target of our work is maximization of the overall average capacity for mobile SUs in coming transmission slots while fulfilling secondary QoS demands, subject to the sum power budget of the SBS and the primary tolerable interference. Therefore, the optimization problem can be formulated as

$$\begin{aligned} \max_{\{x, P\}} & \sum_{j=1}^N \sum_{z=1}^Z x_{j,z} C_{j,z}^{\text{av}} \\ \text{s.t.} & \sum_{j=1}^N \sum_{z=1}^Z x_{j,z} P_{j,z}^S \leq P_{SBS}^{\text{max}}, \end{aligned} \quad (C1)$$

$$\sum_{j=1}^N x_{j,z} I_{j,z}^S \leq I_z^{\text{Th}}, \forall z \quad (C2)$$

$$\overline{\text{SINR}}_{j,z}^{S*}(T_d) \geq \gamma_j^*, \forall j, z \quad (C3)$$

$$P_{j,z}^S \geq 0, \forall j, z \quad (C4)$$

$$\sum_{j=1}^N x_{j,z} \leq 1, \forall z \quad (C5)$$

$$x_{j,z} \in \{0, 1\}, \forall j, z \quad (C6)$$

$$j \in \{1, 2, \dots, N\}, z \in \{1, 2, \dots, Z\}$$

where $x_{j,z}$ is the binary allocation index of SU_j for subchannel z . $x_{j,z}$ is equal to 1 if subchannel z is assigned to SU_j and is 0 otherwise. Accordingly, during the transmitting slot, the downlink average capacity on subchannel z for SU_j is

$$\begin{aligned} C_{j,z}^{\text{av}} &= \frac{1}{T_d} \cdot \int_{t_1}^{t_1+T_d} C_{j,z}^{S*}(t) dt \\ &= \frac{1}{T_d} \int_0^{T_d} B \log_2 \left(1 + SL^2 \cdot \frac{P_{j,z}^S G_j^S(t) d_j^\alpha(t)}{I_{z,j}^P(t) \cdot d_{j,i}^\alpha(t)} \cdot \left(\frac{F_d^{i,j}(v_j, t)}{F_d^j(v_j, t)}\right)^\alpha \right) dt. \end{aligned} \quad (22)$$

In the problem above, the total transmitting power budget of the SBS is denoted by P_{SBS}^{\max} . Thus, the limit on it can be written as (C1). In underlying schemes, SUs are allowed to access the licensed frequency without harmful interference to the PUs' communications. Therefore, the primary SINR demands should be taken into account. The corresponding interference threshold I_z^{Th} in (C2) can be calculated with a primary QoS target β^{Th} :

$$I_z^{Th} = \frac{1}{\beta_i^{Th}} (P_z^P G_{i,z}^P) - N_0 B_0. \quad (23)$$

In mobile CRNs, the SINRs of the SUs are dynamic, whereas the power allocated in a slot is fixed. To ensure that the secondary QoS is satisfactory during the whole transmission slot, $\overline{SINR}_{j,z}^{S*}(T_d)$ is denoted as a statistical SINR criterion for SU_j during the transmission slot $[t_1, t_1+T_d]$ on subchannel z , and we enforce the criterion subject to the constraints (C3). Additionally, regular constraints for subchannel assignment in OFDMA systems are presented as in (C5) and (C6), such that each subchannel is permitted to be assigned to at most one user every time.

From Eq. (22), $SINR_{j,z}^{S*}(t_2)$ can be expressed as

$$\begin{aligned} SINR_{j,z}^{S*}(t_2) &= SL^2 \cdot \frac{P_{j,z}^S G_{j,z}^S(t_1) d_j^\alpha(t_1)}{I_{z,j}^P(t_1) \cdot d_{j,i}^\alpha(t_1)} \cdot \left(\frac{F_d^{i,j}(v_j, t_{21})}{F_d^j(v_j, t_{21})} \right)^\alpha \\ &\propto \left(\frac{F_d^{i,j}(v_j, t_{21})}{F_d^j(v_j, t_{21})} \right)^\alpha \\ &= \left(\frac{\sqrt{d_{AD}^2 + (d_{AB} + v_j t_{21})^2} - 2d_{AD}(d_{AB} + v_j t_{21}) \cos \angle DAB}}{\sqrt{d_{AC}^2 + (d_{AB} + v_j t_{21})^2} - 2d_{AC}(d_{AB} + v_j t_{21}) \cos \angle CAB}} \right)^\alpha \\ &= \left(\frac{v_j^2 t_{21}^2 + 2(d_{AB} - d_{AD} \cos \angle DAB) v_j t_{21} + d_{BD}^2}{v_j^2 t_{21}^2 + 2(d_{AB} - d_{AC} \cos \angle CAB) v_j t_{21} + d_{BC}^2} \right)^{\alpha/2} \end{aligned} \quad (24)$$

Because the referred angles and distances are computable, Eq. (24) could be rewritten as

$$SINR_{j,z}^{S*}(t_2) \propto \frac{v_j^2 t_{21}^2 + a v_j t_{21} + b}{v_j^2 t_{21}^2 + c v_j t_{21} + d} = M(t_{21}), \quad (25)$$

$$\frac{dM(t_{21})}{dt_{21}} = \frac{(c-a)v_j^3 t_{21}^2 + 2(d-b)v_j^2 t_{21} + (ad-bc)v_j}{(v_j^2 t_{21}^2 + c v_j t_{21} + d)^2}, \quad (26)$$

for $t_{21} \in [0, T_{in}^j]$

where v_j is assumed invariable in a transmission slot, and a , b , c , and d are constants that can be calculated easily.

To analyze the monotonicity of the secondary SINR thresholds, we can directly attempt to find the zero points of Eq. (26). As a result, the following equation must be solved:

$$(c-a)v_j^3 t_{21}^2 + 2(d-b)v_j^2 t_{21} + (ad-bc) = 0, \quad t_{21} \in [0, T_{in}^j]. \quad (27)$$

Therefore, we can find the possible zero points $Z(t_{21})$ for Eq. (27) as

if $(d-b)^2 > (c-a)(ad-bc)$:

$$\text{then } Z(t_{21}) = \frac{(b-d) \pm \sqrt{(d-b)^2 - (c-a)(ad-bc)}}{(c-a)}. \quad (28)$$

Note that a and c represent the distance; b and d represent the square of the distance; and T_{in}^j is the actual transmission time of SU_j in one slot. As a result, the absolute values of the possible zero points are usually larger than T_{in}^j . Thus, we assume that $SINR_{j,z}^{S*}$ is approximately monotonous in $[0, T_{in}^j]$. In addition, this assumption will be more reasonable if the transmission slot T_d is shorter.

Thus, $\overline{SINR}_{j,z}^{S*}(T_d)$ can be formulated as a linear function in relation to the values of $SINR_{j,z}^{S*}$ at the beginning and the ending of the slot $[t_1, t_1+T_d]$:

$$\overline{SINR}_{j,z}^{S*}(T_d) = \omega \cdot SINR_{j,z}^{S*}(t_1) + \lambda \cdot SINR_{j,z}^{S*}(t_1 + T_d) \quad (29)$$

where $\omega + \lambda = 1$.

V. PROPOSED ALLOCATION ALGORITHMS

In this section, we propose an efficient subchannel and power allocation algorithm for the downlinks of mobile SUs. Our algorithmic thinking is based on a similar algorithm used in a multi-cell OFDMA-based CRN RA optimization [13], including three steps: power initialization, subchannel assignment and power allocation. Because our scheme focuses on a mobile system, the algorithm should be redesigned as follows.

A. Effective capacity

Different from the spatial and temporal independent capacity for a static CRN suffering slow fading, when the radio resource is going to be allocated for mobile SUs, the dynamic CSI during the whole transmission slot should be reconsidered. Moreover, as SUs leave the coverage of the secondary cell, the resource assigned will no longer be utilized. As a result, we rectify the average effective capacity as follows:

$$\begin{aligned} \overline{C}_{j,z}^{\text{ef}} &= \frac{1}{T_d} \cdot \int_{t_1}^{t_1+T_{in}^j} C_{j,k}^S(t) dt \\ &= \frac{1}{T_d} \int_0^{T_{in}^j} B \log_2 \left\{ 1 + SL^2 \cdot \frac{P_{j,z}^S G_j^S(t_1) d_j^\alpha(t_1)}{I_{z,j}^P(t_1) \cdot d_{j,i}^\alpha(t_1)} \left(\frac{F_d^{i,j}(v_j, t)}{F_d^j(v_j, t)} \right)^\alpha \right\} dt \end{aligned} \quad (30)$$

where T_{in}^j is the actual transmit time of SU_j in the current cell. Obviously, the spectrum efficiency will be higher if T_{in}^j is closer to T_d . Thus, the optimization target of the original problem can be written as

$$\max_{\{x,P\}} \sum_{j=1}^N \sum_{z=1}^Z x_{j,z} \cdot \overline{C}_{j,z}^{\text{ef}}$$

Correspondingly, the $SINR_{j,z}^S$ target can be redefined as

$$\overline{SINR}_{j,z}^{S*}(T_{in}^j) = \omega \cdot SINR_{j,z}^S(t_1) + \lambda \cdot SINR_{j,z}^{S*}(t_1 + T_{in}^j) \quad (31)$$

B. Access control

In our first step, aimed to achieve the secondary initial power, the allowed SUs should satisfy the constraints:

$$d_j(t_1) \leq R \quad \text{and} \quad T_{in}^j \geq \eta T_d, 0 < \eta \leq 1 \quad (C7)$$

Note that this consideration could promote both EE and SE without the resource wasting. In contrast, for the traditional schemes, the power and subchannels might be allocated to the SUs out of the coverage of the assigned SBS during most of their time in the transmission slot. Therefore, with the fixed transmitting slot scheme, a relatively short T_d will increase the SE and EE of the secondary system at a cost of more scheduling operations. The secondary RA scheme referring to an adaptive transmitting slot management would be investigated in our future work and is not be discussed here.

For admitted SU_j , subchannel z is acceptable only if (C2) and (C3) can be fulfilled at the same time. (C2) indicates that the secondary power must be lower than the primary interference threshold. However, (C3) requires the secondary power higher than the secondary SINR threshold. Thus, if the associated constraint (C8)

$$\frac{I_{z,j}^P(t_1) \gamma_j^*}{\left\{ \omega + \lambda \left(\frac{d_j(t_1) F_d^{i,j}(v_j, T_{in})}{d_{j,i}(t_1) F_d^j(v_j, T_{in})} \right)^\alpha \right\} G_j^S(t_1)} \leq SL^2 \frac{I_z^{Th}}{g_{j,z}^S(t_1)}, \quad (C8)$$

cannot be satisfied, then subchannel z is not allowed be assigned to SU_j .

C. Power initialization

Similar to the design in [13], P_{SBS}^{\max} can be divided evenly among the available subchannels for the allowable SUs:

$$P_{\text{equal}} = \frac{P_{SBS}^{\max}}{Z_{\text{actual}}}, \quad (32)$$

where Z_{actual} is the number of accessible subchannels that actually have a chance to be assigned after the access control.

D. Subchannel assignment

In this part, we assume that the power allocation has been accomplished with the power initialization. Thus, the original problem could be simplified as a 0-1 matching problem only concerning subchannel assignment:

$$\begin{aligned} \max_{\{x\}} \quad & \sum_{j=1}^N \sum_{z=1}^Z x_{j,z} \cdot \overline{C}_{j,z}^{\text{ef}} \\ \text{s.t.} \quad & \sum_{j=1}^N x_{j,z} \cdot I_{j,z}^S \leq I_z^{Th}, \forall z \end{aligned} \quad (C9)$$

$$\overline{SINR}_{j,z}^{S*}(T_{in}^j) \geq \gamma_j^*, \forall j, z \quad (C10)$$

$$\sum_{j=1}^N x_{j,z} \leq 1, \forall z \quad (C11)$$

$$\begin{aligned} x_{j,z} &\in \{0, 1\}, \forall j, z \\ j &\in \{1, 2, \dots, N_{\text{actual}}\}, z \in \{1, 2, \dots, Z_{\text{actual}}\} \end{aligned} \quad (C12)$$

where N_{actual} is the number of the actually permitted SUs. The allocated power on any accessible subchannel for allowable SUs is P_{equal} . For our problem here, the Hungarian method [15], the message-passing algorithm [16], or other algorithms that can solve one-to-one assignment problems in polynomial time could be used. These methods have been popularly applied in [14], [16] - [18]; hence, a detailed description is omitted here.

E. Power allocation

In this step, a power allocation algorithm concluding with an enhancement mechanism is presented. According to the subchannel assignment result, the RA problem reduces to

$$\begin{aligned} \max_{\{P\}} \quad & \sum_{j=1}^N \sum_{z=1}^Z \overline{C}_{j,z}^{\text{ef}} \\ \text{s.t.} \quad & \sum_{j \in \mathbf{A}} \sum_{z \in \mathbf{n}_j} P_{j,z}^S \leq P_{SBS}^{\max}, \forall j, z \end{aligned} \quad (C13)$$

$$\begin{aligned} \overline{SINR}_{j,z}^{S*}(T_{in}^j) &\geq \gamma_j^*, \forall j, z \\ j &\in \{1, 2, \dots, N_{\text{actual}}\}, z \in \{1, 2, \dots, Z_{\text{actual}}\} \end{aligned} \quad (C14)$$

where \mathbf{n}_j is the set of the subchannels assigned to SU_j , and \mathbf{A} is the set of admitted SUs. To maximize the overall average EC, first, the minimum power required by SU_j on subchannel z should be allocated according to (C14). If the power is denoted as $P_{j,z}^{S_{\min}}$, then

$$P_{j,z}^{S_{\min}} = \arg \min_{P_{j,z}^S} \left\{ \overline{SINR}_{j,z}^{S*}(T_{in}^j) \right\}. \quad (33)$$

Because (C13) and (C14) cannot be guaranteed at the same time,

$$\sum_{j \in \mathbf{A}} \sum_{z \in \mathbf{n}_j} P_{j,z}^{S_{\min}} > P_{SBS}^{\max}, \quad (34)$$

the assigned subchannels with the highest minimum power demand are excluded one by one until the total minimum power on the remaining accessible subchannels does not exceed the budget.

Thus, the remaining power allocated for SU_j on subchannel z could be denoted by $P_{j,z}^{S_{\text{wf}}}$. Thus, the solution of the reduced power allocation problem

$$\begin{aligned} \max_{\{P\}} & \sum_{j=1}^N \sum_{z=1}^Z \overline{C_{j,z}^{ef}} \\ \text{s.t.} & \sum_{j \in \mathbf{A}} \sum_{z \in \mathbf{n}_j} (P_{j,z}^{S_fw} + P_{j,z}^{S_min}) \leq P_{SBS}^{\max}, \forall j, z \quad (C13) \\ & j \in \{1, 2, \dots, N_{\text{actual}}\}, z \in \{1, 2, \dots, Z_{\text{actual}}\} \end{aligned}$$

is a water-filling (WF) processing given by

$$P_{j,z}^{S_fw} = \left[\omega - \frac{1}{\text{SINR}_{j,z}^{S^*}(T_{in}^j)} \right]^+, \quad (35)$$

where Z_{actual} is the number of assigned subchannels constrained by (C13) and (C14). $[x]^+ = \max\{0, x\}$, and ω is set to ensure

$$\sum_{j \in \mathbf{A}} \sum_{z \in \mathbf{n}_j} P_{j,z}^{S_fw} = P_{SBS}^{\max} - \sum_{j \in \mathbf{A}} \sum_{z \in \mathbf{n}_j} P_{j,z}^{S_min} \quad (36)$$

Moreover, ω can be approximately calculated as in Eq. (37) for most cases:

$$\omega = \frac{1}{Z_{\text{actual}}} \left(P_{SBS}^{\max} - \sum_{j \in \mathbf{A}} \sum_{z \in \mathbf{n}_j} P_{j,z}^{S_min} + \sum_{j \in \mathbf{A}} \sum_{z \in \mathbf{n}_j} \frac{1}{\text{SINR}_{j,z}^{S^*}(T_{in}^j)} \right). \quad (37)$$

Therefore, the total power allocated is

$$P_{j,z}^{S^*} = P_{j,z}^{S_fw} + P_{j,z}^{S_min}. \quad (38)$$

In addition, if the interference constraints (C9) can be satisfied for all PUs, then the RA solution can be determined directly, and the power allocation vector can be denoted as $P^{S^*} = \{P_{j,z}^{S^*}\}$. Otherwise, a power enhancement step should be conducted iteratively, referring to [13].

The combination of the steps above represents the complete algorithm. It can be concluded that this algorithm is decentralized and cooperatively employed on both sides of the SBS and the mobile SUs.

F. Complexity analysis

The complexity of the innovative algorithm is dominated by the operations for the matching algorithm in the subchannel assignment step. Taking the use of the Hungarian algorithm as an example, the total complexity of the stepwise algorithm above is no more than $O(N_{\text{actual}}^3)$ [13].

G. General model extension

In the work above, we proposed an RA method for mobile SUs with an assumption of static PUs. Furthermore, if the location and MSI of the PUs can be acquired by CRN as well, then the RA scheme can be extended to a general scene, where both SUs and PUs are moving at the same time. In detail, the system model can be depicted as follows:

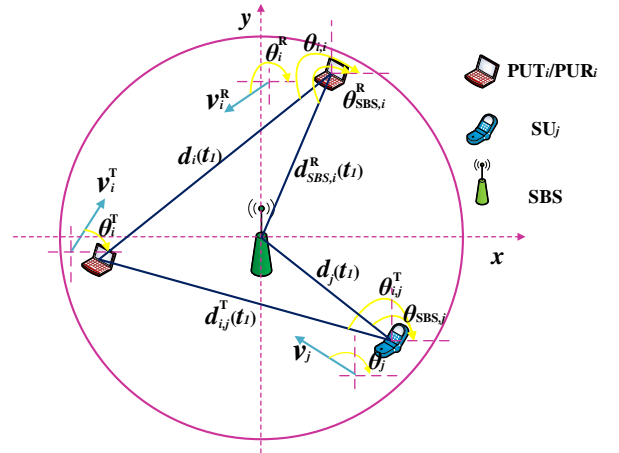


Figure 2. General Mobile CRN system model.

Considering the model more simply and practically, the speeds of PUs are assumed as relatively low compared with the SUs'. Thus, the shadow fading for PUs is assumed fixed during a SU's slot. Otherwise, a similar compensation parameter SL' will be used to predict the primary CSI:

$$G_{i,z}^{P^*}(t_2) = SL' \cdot \mathbf{E}[G_{i,z}^P(t_2)] \quad (39)$$

where $0 < SL' < 1$. Thus, the interference power from a moving PUT to a moving SU and the corresponding CSI can be predicted according to the following strategy.

Case 1: if PUT is mobile while PUR is static, the corresponding MSI can be calculated according to Fig. 2:

$$\begin{aligned} d_i(t_2) &= \sqrt{\left(d_i(t_1) \cos \theta_{i,i} - v_i^T t_{21} \cos \theta_i^T \right)^2 + \left(d_i(t_1) \sin \theta_{i,i} - v_i^T t_{21} \sin \theta_i^T \right)^2} \\ &\stackrel{\text{def}}{=} F_d^{\text{Ti,Ri}}(v_i^T, t_{21}) \end{aligned} \quad (40)$$

$$\begin{aligned} d_j(t_2) &= \sqrt{\left(d_j(t_1) \cos \theta_{SBS,j} - v_j t_{21} \cos \theta_j \right)^2 + \left(d_j(t_1) \sin \theta_{SBS,j} - v_j t_{21} \sin \theta_j \right)^2} \\ &\stackrel{\text{def}}{=} F_d^j(v_j, t_{21}) \end{aligned} \quad (41)$$

$$\begin{aligned} d_{i,j}^T(t_2) &= \sqrt{\left\{ d_{i,j}^T(t_1) \cos \theta_{i,j}^T - (v_j \cos \theta_j - v_i^T \cos \theta_i^T) t_{21} \right\}^2 + \left\{ d_{i,j}^T(t_1) \sin \theta_{i,j}^T - (v_j \sin \theta_j - v_i^T \sin \theta_i^T) t_{21} \right\}^2} \\ &\stackrel{\text{def}}{=} F_d^{\text{Ti,j}}(v_j, v_i^T, t_{21}) \end{aligned} \quad (42)$$

where $d_i(t_1)$, $d_j(t_1)$, and $d_{i,j}^T(t_1)$ are the distances of the links PUT_i-PUR_i, SBS-SU_j, and PUT_i-SU_j, respectively, at t_1 , and θ_i , $\theta_{SBS,j}$, and $\theta_{i,j}^T$ are the corresponding angles between the links and the horizontal axis. Moreover, v_i^T denotes the speed of PUT_i and θ_i^T is its drift angle.

Because the transmission power of PU_i is unchanged, the interference it introduces to SU_j at t_2 can be calculated as

$$I_{z,j}^{P*}(t_2) = \frac{1}{SL} \cdot \mathbf{E}[I_{z,j}^P(t_2)] \quad (43)$$

$$\approx \frac{1}{SL} \cdot \left(\frac{d_{i,j}^T(t_1)}{F_d^{Ti,j}(v_j, v_i^T, t_{21})} \right)^\alpha I_{z,j}^P(t_1).$$

Similarly, the power gain between the SBS and SU_j can be deduced as

$$G_{j,z}^{S*}(t_2) = SL \cdot \left(\frac{d_j(t_1)}{F_d^j(v_j, t_{21})} \right)^\alpha G_{j,z}^S(t_1). \quad (44)$$

Combining Eq. (43) and Eq. (44), when the PUT_i is moving, the capacity for SU_j on subchannel z at t₂ is

$$C_{j,z}^{S*}(t_2) \approx B_0 \log_2 \left(1 + \frac{G_{j,z}^{S*}(t_2) P_{j,z}^S}{I_{z,j}^{P*}(t_2)} \right)$$

$$= B_0 \log_2 \left(1 + SL^2 \cdot \frac{\left(\frac{d_j(t_1)}{F_d^j(v_j, t_{21})} \right)^\alpha G_{j,z}^S(t_1) P_{j,z}^S}{\left(\frac{d_{i,j}^T(t_1)}{F_d^{Ti,j}(v_j, v_i^T, t_{21})} \right)^\alpha I_{z,j}^P(t_1)} \right)$$

$$= B \log_2 \left(1 + SL^2 \cdot \frac{P_{j,z}^S G_{j,z}^S(t_1) d_j^\alpha(t_1)}{I_{z,j}^P(t_1) \cdot \{d_{i,j}^T(t_1)\}^\alpha} \cdot \left(\frac{F_d^{Ti,j}(v_j, v_i^T, t_{21})}{F_d^j(v_j, t_{21})} \right)^\alpha \right) \quad (45)$$

where SINR_{j,z}^{S*}(t₂) is expressed in Eq. (46). Accordingly, we can similarly define the secondary SINR target as

$$\overline{\text{SINR}}_{j,z}^{S*}(T_{in}^j) = \omega \cdot \text{SINR}_{j,z}^S(t_1) + \lambda \cdot \text{SINR}_{j,z}^{S*}(t_1 + T_{in}^j), \quad (47)$$

which should satisfy the secondary QoS demands as in C(3):

$$\overline{\text{SINR}}_{j,z}^{S*}(T_{in}^j) \geq \gamma_j^*. \quad (48)$$

In addition, the primary interference thresholds must be calculated, as those in C(2). Because the PURs are static, the

$$\text{SINR}_{j,z}^{S*}(t_2) = SL^2 \cdot \frac{P_{j,z}^S G_{j,z}^S(t_1) d_j^\alpha(t_1)}{I_{z,j}^P(t_1) \cdot \{d_{i,j}^T(t_1)\}^\alpha} \cdot \left(\frac{F_d^{Ti,j}(v_j, v_i^T, t_{21})}{F_d^j(v_j, t_{21})} \right)^\alpha \left(\frac{F_d^{Ti,j}(v_j, v_i^T, t_{21})}{F_d^j(v_j, t_{21})} \right)^\alpha$$

$$= \left(\frac{\sqrt{\{d_{i,j}^T(t_1) \cos \theta_{i,j}^T - (v_j \cos \theta_j - v_i^T \cos \theta_i^T) t_{21}\}^2 + \{d_{i,j}^T(t_1) \sin \theta_{i,j}^T - (v_j \sin \theta_j - v_i^T \sin \theta_i^T) t_{21}\}^2}}{\sqrt{\{d_j(t_1) \cos \theta_{\text{SBS},j} - v_j t_{21} \cos \theta_j\}^2 + \{d_j(t_1) \sin \theta_{\text{SBS},j} - v_j t_{21} \sin \theta_j\}^2}} \right)^\alpha$$

$$= \left(\frac{\left\{ v_j^2 + (v_i^T)^2 - v_j v_i^T \cos(\theta_j - \theta_i^T) \right\} t_{21}^2 - 2d_{i,j}^T(t_1) \{ \cos \theta_{i,j}^T (v_j \cos \theta_j - v_i^T \cos \theta_i^T) \} t_{21}}{v_j^2 t_{21}^2 - 2d_j(t_1) v_j \cos(\theta_{\text{SBS},j} - \theta_j) t_{21} + d_j^2(t_1)} \right)^{\alpha/2}$$

$$+ \frac{-2d_{i,j}^T(t_1) \{ \sin \theta_{i,j}^T (v_j \sin \theta_j - v_i^T \sin \theta_i^T) \} t_{21} + \{d_{i,j}^T(t_1)\}^2}{v_j^2 t_{21}^2 - 2d_j(t_1) v_j \cos(\theta_{\text{SBS},j} - \theta_j) t_{21} + d_j^2(t_1)}$$

$$\stackrel{\text{def}}{=} \left(\frac{A(v_j, v_i^T) t_{21}^2 + B(v_j, v_i^T) t_{21} + C}{D(v_j) t_{21}^2 + E(v_j) t_{21} + F} \right)^{\alpha/2}, \quad (46)$$

power gains of the interference links between them and SBS (i.e., g_{j,z}^S) are constant. Thus, the interference the PURs suffering (i.e., I_{j,z}^S) during a secondary transmission slot are constant as well. Regarding the PUs' interference thresholds, the secondary system should take more consideration of the primary QoS loss caused by the PUTs' mobility. Therefore, to protect the primary transmission during the whole slot, we define the primary interference threshold as follows:

$$I_{j,z}^{\text{Th}} = \min \{ I_{j,z}^{\text{Th}}(t_2) \}, t_{21} \in [0, T_{in}^j] \quad (49)$$

$$I_{j,z}^{\text{Th}}(t_2) = \frac{P_z^P G_{i,z}^P(t_2)}{\beta_i^{\text{Th}}} - N_0 B_0. \quad (50)$$

where

$$G_{i,z}^{P*}(t_2) = \left(\frac{d_i(t_1)}{F_d^{Ti,Ri}(v_i^T, t_{21})} \right)^\alpha \cdot G_{i,z}^P(t_1)$$

$$= \left(\frac{d_i^2(t_1)}{\{v_i^T\}^2 t_{21}^2 - 2d_i(t_1) v_i^T \cos(\theta_{i,i} - \theta_i^T) t_{21} + d_i^2(t_1)} \right)^{\alpha/2} \cdot G_{i,z}^P(t_1) \quad (51)$$

and G_{i,z}^P(t₁) is measurable. As a result, I_{j,z}Th = I_{j,z}Th(t₂₁^{max}) where

$$t_{21}^{\text{max}} = \arg \max_{t_{21}} \left\{ \frac{\{v_i^T\}^2 t_{21}^2 - 2d_i(t_1) v_i^T \cos(\theta_{i,i} - \theta_i^T) t_{21}}{+d_i^2(t_1)}, |t_{21} \in [0, T_{in}^j] \right\}. \quad (52)$$

Because

$$\left\{ v_i^T \right\}^2 t_{21}^2 - 2d_i(t_1) v_i^T \cos(\theta_{i,i} - \theta_i^T) t_{21} + d_i^2(t_1) \geq \left\{ v_i^T t_{21} - d_i(t_1) \right\}^2 \geq 0,$$

we can easily obtain

$$t_{21}^{\max} = \begin{cases} 0, & \text{if } \frac{T_{in}^j}{2} < \frac{d_i(t_1) \cos(\theta_{i,i} - \theta_i^T)}{v_i^T} \\ T_{in}^j, & \text{else} \end{cases} \quad (53)$$

As a result, the secondary power should be constrained by the primary interference thresholds as:

$$P_{j,z}^S \leq \left(\frac{d_i(t_1)}{F_d^{Ti,Ri}(v_i^T, t_{21})} \right)^\alpha \cdot \frac{P_z^P G_{i,z}^P(t_1)}{\beta_i^{Th} g_{j,z}^S(t_1)} \left| \frac{N_0 B_0}{g_{j,z}^S(t_1)} \right|_{t_{21}} = \begin{cases} 0, & \text{if } \frac{T_{in}^j}{2} < \frac{d_i(t_1) \cos(\theta_{i,i} - \theta_i^T)}{v_i^T} \\ T_{in}^j, & \text{else} \end{cases} \quad (54)$$

Combining C(7), Eq. (43) and Eq. (49), the access control criterion can be obtained for *Case 1* as C(7) and

$$\frac{I_{z,j}^P(t_1) \gamma_j^*}{\left\{ \omega + \lambda SL^2 \left(\frac{d_j(t_1) F_d^{Ti,j}(v_j, v_i^T, T_{in}^j)}{d_{i,j}^T(t_1) F_d^j(v_j, T_{in}^j)} \right)^\alpha \right\} G_{j,z}^S(t_1)} \leq \left(\frac{d_i(t_1)}{F_d^{Ti,Ri}(v_i^T, t_{21}^*)} \right)^\alpha \cdot \frac{P_z^P G_{i,z}^P(t_1)}{\beta_i^{Th} g_{j,z}^S(t_1)} - \frac{N_0 B_0}{g_{j,z}^S(t_1)} \quad (55)$$

where t_{21}^* can be calculated by Eq. (52).

After accomplishing the analyses above, an optimization problem can be formulated referring to that in Section IV,

$$P_{j,z}^P \leq \frac{P_z^P \left(\frac{d_i(t_1) F_d^{SBS,Ri}(v_i^R, t_{21})}{d_{SBS,i}^R(t_1) F_d^{Ti,Ri}(v_i^R, t_{21})} \right)^\alpha G_{i,z}^P(t_1)}{g_{j,z}^S(t_1) \beta_i^{Th}} - \frac{N_0 B_0}{g_{j,z}^S(t_1)} \left(\frac{F_d^{SBS,Ri}(v_i^R, t_{21})}{d_{SBS,i}^R(t_1)} \right)^\alpha$$

$$< \frac{P_z^P \left(\frac{d_i(t_1) F_d^{SBS,Ri}(v_i^R, t_{21})}{d_{SBS,i}^R(t_1) F_d^{Ti,Ri}(v_i^R, t_{21})} \right)^\alpha G_{i,z}^P(t_1)}{g_{j,z}^S(t_1) \beta_i^{Th}} = \left(\frac{F_d^{SBS,Ri}(v_i^R, t_{21})}{F_d^{Ti,Ri}(v_i^R, t_{21})} \right)^\alpha \left\{ \frac{P_z^P \left(\frac{d_i(t_1)}{d_{SBS,i}^R(t_1)} \right)^\alpha G_{i,z}^P(t_1)}{g_{j,z}^S(t_1) \beta_i^{Th}} \right\}$$

$$= \left(\frac{\left(d_{SBS,i}^R(t_1) \cos \theta_{SBS,i}^R - v_i^R t_{21} \cos \theta_i^R \right)^2 + \left(d_{SBS,i}^R(t_1) \sin \theta_{SBS,i}^R - v_i^R t_{21} \sin \theta_i^R \right)^2}{\left(d_i(t_1) \cos \theta_{i,i} - v_i^R t_{21} \cos \theta_i^R \right)^2 + \left(d_i(t_1) \sin \theta_{i,i} - v_i^R t_{21} \sin \theta_i^R \right)^2} \right)^{\alpha/2} \cdot \left\{ \frac{P_z^P \left(\frac{d_i(t_1)}{d_{SBS,i}^R(t_1)} \right)^\alpha G_{i,z}^P(t_1)}{g_{j,z}^S(t_1) \beta_i^{Th}} \right\}$$

$$= \left(\frac{\left\{ v_i^R \right\}^2 t_{21}^2 - 2 d_{SBS,i}^R(t_1) v_i^R \cos(\theta_{SBS,i}^R - \theta_i^R) t_{21} + \left\{ d_{SBS,i}^R(t_1) \right\}^2}{\left\{ v_i^R \right\}^2 t_{21}^2 - 2 d_i(t_1) v_i^R \cos(\theta_{i,i} - \theta_i^R) t_{21} + \left\{ d_i(t_1) \right\}^2} \right)^{\alpha/2} \cdot \left\{ \frac{P_z^P \left(\frac{d_i(t_1)}{d_{SBS,i}^R(t_1)} \right)^\alpha G_{i,z}^P(t_1)}{g_{j,z}^S(t_1) \beta_i^{Th}} \right\}$$

$$\stackrel{def}{=} \left(\frac{\left\{ v_i^R \right\}^2 t_{21}^2 + a' v_i^R t_{21} + b'}{\left\{ v_i^R \right\}^2 t_{21}^2 + c' v_i^R t_{21} + d'} \right)^{\alpha/2} \stackrel{def}{=} F_i^R(t_{21})^{\alpha/2} e', \quad (63)$$

solved using an algorithm similar to that originally proposed for the static primary system.

Case 2: if PUR is mobile while PUT is static, then $v_i^T=0$ and $v_i^R>0$. Therefore, the power gains of the interference links between them and SBS are varying. The corresponding MSI and CSI can be predicted as

$$d_{SBS,i}^R(t_2) = \sqrt{\left(d_{SBS,i}^R(t_1) \cos \theta_{SBS,i}^R - v_i^R \cos \theta_i^R t_{21} \right)^2 + \left(d_{SBS,i}^R(t_1) \sin \theta_{SBS,i}^R - v_i^R \sin \theta_i^R t_{21} \right)^2} \stackrel{def}{=} F_d^{SBS,Ri}(v_i^R, t_{21}), \quad (56)$$

$$g_{j,z}^{S*}(t_2) = \left(\frac{d_{SBS,i}^R(t_1)}{F_d^{SBS,Ri}(v_i^R, t_{21})} \right)^\alpha g_{j,z}^S(t_1). \quad (57)$$

Thus, the corresponding interference SU_j introducing can be predicted as

$$I_{j,z}^{S*}(t_2) = g_{j,z}^{S*}(t_2) P_{j,z}^S, \quad (58)$$

and the primary interference constraints should be satisfied as

$$I_{j,z}^{S*}(t_2) \leq I_{j,z}^{Th}(t_2), \forall z \in \{1, 2, \dots, Z\}, t_2 \in [t_1, t_1 + T_{in}^j], \quad (59)$$

where

$$P_{j,z}^S < \min \left\{ \frac{P_z^P \left(\frac{d_i(t_1) F_d^{\text{SBS,Ri}}(v_i^R, 0)}{d_{\text{SBS},i}^R(t_1) F_d^{\text{Ti,Ri}}(v_i^R, 0)} \right)^\alpha G_{i,z}^P(t_1)}{g_{j,z}^S(t_1) \beta_i^{\text{Th}}}, \frac{P_z^P \left(\frac{d_i(t_1) F_d^{\text{SBS,Ri}}(v_i^R, T_j^{\text{in}})}{d_{\text{SBS},i}^R(t_1) F_d^{\text{Ti,Ri}}(v_i^R, T_j^{\text{in}})} \right)^\alpha G_{i,z}^P(t_1)}{g_{j,z}^S(t_1) \beta_i^{\text{Th}}} \right\} \quad (64)$$

$$P_{j,z}^S \leq \min \left\{ \frac{P_z^P \left(\frac{d_i(t_1) F_d^{\text{SBS,Ri}}(v_i^R, 0)}{d_{\text{SBS},i}^R(t_1) F_d^{\text{Ti,Ri}}(v_i^R, 0)} \right)^\alpha G_{i,z}^P(t_1)}{g_{j,z}^S(t_1) \beta_i^{\text{Th}}} - \frac{N_0 B_0 \left(\frac{F_d^{\text{SBS,Ri}}(v_i^R, 0)}{d_{\text{SBS},i}^R(t_1)} \right)^\alpha}{g_{j,z}^S(t_1)}, \frac{P_z^P \left(\frac{d_i(t_1) F_d^{\text{SBS,Ri}}(v_i^R, T_j^{\text{in}})}{d_{\text{SBS},i}^R(t_1) F_d^{\text{Ti,Ri}}(v_i^R, T_j^{\text{in}})} \right)^\alpha G_{i,z}^P(t_1)}{g_{j,z}^S(t_1) \beta_i^{\text{Th}}} - \frac{N_0 B_0 \left(\frac{F_d^{\text{SBS,Ri}}(v_i^R, T_j^{\text{in}})}{d_{\text{SBS},i}^R(t_1)} \right)^\alpha}{g_{j,z}^S(t_1)} \right\}, \quad (65)$$

$$I_{j,z}^{\text{Th}}(t_2) = \frac{P_z^P G_{i,z}^P(t_2)}{\beta_i^{\text{Th}}} - N_0 B_0. \quad (60)$$

According to Eq. (40), the following is obtained:

$$d_i(t_2) = \sqrt{\left(d_i(t_1) \cos \theta_{i,i} - v_i^R t_{21} \cos \theta_i^R \right)^2 + \left(d_i(t_1) \sin \theta_{i,i} - v_i^R t_{21} \sin \theta_i^R \right)^2} \quad (61)$$

$$\stackrel{\text{def}}{=} F_d^{\text{Ti,Ri}}(v_i^R, t_{21}),$$

$$G_{i,z}^P(t_2) = \left(\frac{d_i(t_1)}{F_d^{\text{Ti,Ri}}(v_i^R, t_{21})} \right)^\alpha G_{i,z}^P(t_1)$$

$$= \left(\frac{d_i^2(t_1)}{\left\{ v_i^R \right\}^2 t_{21}^2 - 2d_i(t_1)v_i^R \cos(\theta_{i,i} - \theta_i^R)t_{21} + d_i^2(t_1)} \right)^{\alpha/2} G_{i,z}^P(t_1). \quad (62)$$

Consequently, combining Eqs. (57)- (62), the secondary power must satisfy the constraint Eq. (63) on the previous page, where e' is a constant.

Because $F_i^R(t_{21})$ is monotonous according to Eq. (24), the interference constraints on secondary power can be transformed as Eq. (64) at the top of the page. For convenience and practical application, the constraints can be approximately simplified as Eq. (65) or Eq. (66).

$$\text{SINR}_{j,z}^{S*}(t_2) \propto \left(\frac{F_d^{\text{Ti,j}}(v_j, t_{21})}{F_d^j(v_j, t_{21})} \right)^\alpha$$

$$= \left(\frac{\sqrt{\left\{ d_{i,j}^T(t_1) \cos \theta_{i,j}^T - v_j \cos \theta_j t_{21} \right\}^2 + \left\{ d_{i,j}^T(t_1) \sin \theta_{i,j}^T - v_j \sin \theta_j t_{21} \right\}^2}}{\sqrt{\left(d_j(t_1) \cos \theta_{\text{SBS},j} - v_j \cos \theta_j t_{21} \right)^2 + \left(d_j(t_1) \sin \theta_{\text{SBS},j} - v_j \sin \theta_j t_{21} \right)^2}} \right)^\alpha \quad (71)$$

$$= \left(\frac{v_j^2 t_{21}^2 - 2d_{i,j}^T(t_1)v_j \cos(\theta_{i,j}^T - \theta_j)t_{21} + \left\{ d_{i,j}^T(t_1) \right\}^2}{v_j^2 t_{21}^2 - 2d_j(t_1)v_j \cos(\theta_{\text{SBS},j} - \theta_j)t_{21} + d_j^2(t_1)} \right)^{\alpha/2},$$

$$P_{j,z}^S \leq \min \left\{ \frac{P_z^P \left(\frac{d_i(t_1) F_d^{\text{SBS,Ri}}(v_i^R, 0)}{d_{\text{SBS},i}^R(t_1) F_d^{\text{Ti,Ri}}(v_i^R, 0)} \right)^\alpha G_{i,z}^P(t_1)}{g_{j,z}^S(t_1) \beta_i^{\text{Th}}} - \frac{N_0 B_0}{g_{j,z}^S(t_1)}, \frac{P_z^P \left(\frac{d_i(t_1) F_d^{\text{SBS,Ri}}(v_i^R, T_j^{\text{in}})}{d_{\text{SBS},i}^R(t_1) F_d^{\text{Ti,Ri}}(v_i^R, T_j^{\text{in}})} \right)^\alpha G_{i,z}^P(t_1)}{g_{j,z}^S(t_1) \beta_i^{\text{Th}}} - \frac{N_0 B_0}{g_{j,z}^S(t_1)} \right\}. \quad (66)$$

According to Eq. (57) and Eq. (58) the interference SUs suffering can be predicted as

$$I_{z,j}^{P*}(t_2) = \frac{1}{SL} \cdot \left(\frac{d_{i,j}^T(t_1)}{F_d^{\text{Ti,j}}(v_j, t_{21})} \right)^\alpha I_{z,j}^P(t_1) \quad (67)$$

where

$$F_d^{\text{Ti,j}}(v_j, t_{21}) = \sqrt{\left\{ d_{i,j}^T(t_1) \cos \theta_{i,j}^T - v_j \cos \theta_j t_{21} \right\}^2 + \left\{ d_{i,j}^T(t_1) \sin \theta_{i,j}^T - v_j \sin \theta_j t_{21} \right\}^2}. \quad (68)$$

As a result, the predicted value of the SINR for SU_j on subchannel z at t_2 can be expressed as

$$\text{SINR}_{j,z}^{S*}(t_2) = SL^2 \cdot \frac{P_{j,z}^S G_{j,z}^S(t_1) d_j^\alpha(t_1)}{I_{z,j}^P(t_1) \cdot \left\{ d_{i,j}^T(t_1) \right\}^\alpha} \cdot \left(\frac{F_d^{\text{Ti,j}}(v_j, t_{21})}{F_d^j(v_j, t_{21})} \right)^\alpha, \quad (69)$$

and the corresponding Shannon capacity is Eq. (70) on the next page.

$$C_{j,z}^{S*}(t_2) = B \log_2 \left(1 + SL^2 \cdot \frac{P_{j,z}^S G_{j,z}^S(t_1) d_j^\alpha(t_1)}{I_{z,j}^P(t_1) \cdot \{d_{i,j}^T(t_1)\}^\alpha} \cdot \left(\frac{F_d^{Ti,j}(v_j, t_{21})}{F_d^j(v_j, t_{21})} \right)^\alpha \right) \quad (70)$$

As shown in Eq. (71), we can similarly reach the SINR target for SU_j on subchannel z during [t₁, t₁+T_d] as

$$\overline{SINR}_{j,z}^{S*}(T_{in}^j) = \omega \cdot SINR_{j,z}^S(t_1) + \lambda \cdot SINR_{j,z}^{S*}(t_1 + T_{in}^j) \quad (72)$$

As a result, the access control criterion for *Case 2* can be deduced as C(7) and

$$\leq \min \left\{ \begin{array}{l} \frac{I_{z,j}^P(t_1) \gamma_j^*}{\omega + \lambda SL^2 \left(\frac{d_j(t_1) F_d^{Ti,j}(v_j, T_{in}^j)}{d_{i,j}^T(t_1) F_d^j(v_j, T_{in}^j)} \right)^\alpha} G_{j,z}^S(t_1)} \\ \frac{P_z^P \left(\frac{d_i(t_1) F_d^{SBS,Ri}(v_i^R, 0)}{d_{SBS,i}^R(t_1) F_d^{Ti,Ri}(v_i^R, 0)} \right)^\alpha G_{i,z}^P(t_1)}{g_{j,z}^S(t_1) \beta_i^{Th}} \frac{N_0 B_0}{g_{j,z}^S(t_1)}}, \\ \frac{P_z^P \left(\frac{d_i(t_1) F_d^{SBS,Ri}(v_i^R, T_{in}^{in})}{d_{SBS,i}^R(t_1) F_d^{Ti,Ri}(v_i^R, T_{in}^{in})} \right)^\alpha G_{i,z}^P(t_1)}{g_{j,z}^S(t_1) \beta_i^{Th}} \frac{N_0 B_0}{g_{j,z}^S(t_1)} \end{array} \right\} \quad (73)$$

After the analyses above, the RA problem formulation and the algorithm design can be accomplished in a similar manner to that in Section 4. Moreover, by combining the analyses in *Case 1* and *Case 2*, the resource allocation algorithm could be easily reached for the condition where the PUs and PURs are moving at the same time. As a result, it will not be individually discussed here.

Last, note that the RA schemes related to the moving PUs are extended with the same steps as the original proposed scheme, except for the use of different CSI to conduct access control and power allocation. Moreover, the primary mobility clearly only makes it more difficult for secondary networks to predict the CSI and access the spectrum. As a result, the descriptions of the general schemes are only roughly provided, and more attention is paid to the performance analyses of the original one without considering the effect of the primary speed.

VI. Simulation results

In this section, the performance of the proposed algorithm related to static PUs is evaluated via simulations, and then, we compare the proposed algorithm with some other RA schemes.

An OFDMA-based cellular CRN with M pairs of PUs and an SBS, N SUs, is considered. The minimum radius of the CRN coverage is R=500 m. The number of subchannels each PU provides is set to 4, and the bandwidth is equally fixed as 0.3125 MHz. We assume that the PUs and SUs appear randomly in the cell. The location information of the SUs can be transmitted to the SBS together with the sensing report in sensing slots. The transmit power of every PU is fixed as **1 W/2 W/4 W**, the total power budget of SBS is **1 W/4 W/8 W**, and the power spectral density of the noise is 5×10^{-20}

W/Hz. The slow fading channel is modeled as a Rayleigh multipath channel, and the pass-loss exponent α is set to 4. The sensing duration of all SUs is 1 ms, and SUs sense every 2 s [9]. Considering that the sensing duration is short, the SUs' locations are assumed unchanged during the sensing slot. With the thinking of invariable direction and speed, the duration of the transmission slot is set as T_d=10 s, and $\eta=0.8$. The heading angles of SUs are assumed to be uniformly distributed between 0 and 2π , and their speeds are chosen from 0 to 40 m/s. To investigate the performance lower bound of our anti-shadowing RA scheme, we assume that the decorrelation distance of the shadow fading in the simulated cell is very short, i.e., $x_{\sigma}^{SU_{j,z}}(t_1)$ and $x_{\sigma}^{SU_{j,z}}(t_2)$ are assumed to be independent during the transmission slots, and the standard deviation σ_{XY} is set as **4 dB/8 dB/12 dB**.

Because no studies on similar RA schemes for mobile CRNs are found in the existing works, our work cannot be rigorously compared with the existing literature. However, researchers have provided a power control scheme with fixed channel assignment in [5] and a spectrum access scheme with fixed power allocation in [6]. As a result, we plan to consider four schemes referring to traditional works according to the analysis in [13]. The compared schemes are listed in Table 1. According to (13), the CSI prediction takes the expectation of $G_{j,z}^S$ at t_2 multiplied by SL as the actual value; the performance for both the secondary system will be unable to achieve the ideal results. Therefore, the performances of the schemes employing ideal CSI predicting results (i.e., Ideal Proposed Scheme and Ideal Scheme III) are simulated as well. It will help evaluate the accuracy of the CSI prediction and the study of advanced anti-shadowing predicting methods, such as those based on the vehicle-to-vehicle (V2V) helped CSI tracking and deep learning assisted prediction.

TABLE I
FIVE TESTED SCHEMES

Schemes	Subchannel Allocation	Power Allocation
Proposed I	proposed CSI-method blind	proposed WF-method equal
II	instantaneous sensing based	equal
III	proposed CSI-method	equal
IV	instantaneous sensing based	proposed WF-method

Fig. 3 illustrates the total average effective capacity of all mobile SUs for different schemes. In Fig. 3(a), first note that the faster the SUs move, the lower total average effective capacity is because the SUs' probability of moving beyond the cell during the transmitting slot is higher, and more SUs are refused for the Scheme Proposed and Scheme III. However, the subchannels are allocated without considering the secondary speed for the other schemes, leading to more resources wasted and lower effective capacity. Fig. 3(b), the increasing secondary SINR target is unable to improve the effective capacity and decreases obviously as the SINR target gets higher than -5 dB. This phenomenon originates

from the primary interference limit and the secondary power budget as in (C8). Moreover, the performance changes in Fig. 3(d) are caused by the former factor as well.

According to Fig. 3(c), the capacity for our original proposed scheme clearly becomes higher with an increasing N when N is not so large (from 2 to 16). However, there exists no obvious increase when N becomes larger (from 16 to 32) because when N increases, the subchannels and power are allocated more reasonably in our originally proposed scheme. In contrast, the secondary effective capacity becomes worse as N increases for the instantaneous sensing result based schemes (i.e., Scheme II and IV). In particular, the newly proposed scheme is found to provide a significant higher total average effective capacity for the secondary system. Specifically, note that this capacity improvement originates from not only the anti-shadowing CSI predicting based average SINR definition but also the joint access control step and the enhanced power allocation scheme. In addition, through the total effective capacity for the Ideal Scheme Proposed and Scheme III, it is found that more advanced CSI predicting methods need to be explored because the prediction results here are perfect only if the

shadowing correlation coefficients remain 0 all the time. The secondary power and subchannel utilization ratios are shown in Fig. 4 and Fig. 5, respectively. Aiming to evaluate the secondary EE for the schemes compared, the effective power is defined as the useful power allocated to the admitted SUs on valid subchannels. Thus, the power utilization ratio could be defined by the ratio of the effective power to the total power allocated. According to Fig. 4(a), the effective power ratios of the anti-shadowing CSI predicting based schemes (i.e., Scheme Proposed and Scheme III) remain stable when the SUs move faster. This stability occurs because such schemes are guided by the predicting results to avoid wasting power on the SUs beyond the coverage of the current cell, resulting in a similar gain for the secondary SE according to Fig. 5(a). Moreover, these benefits mentioned are promoted

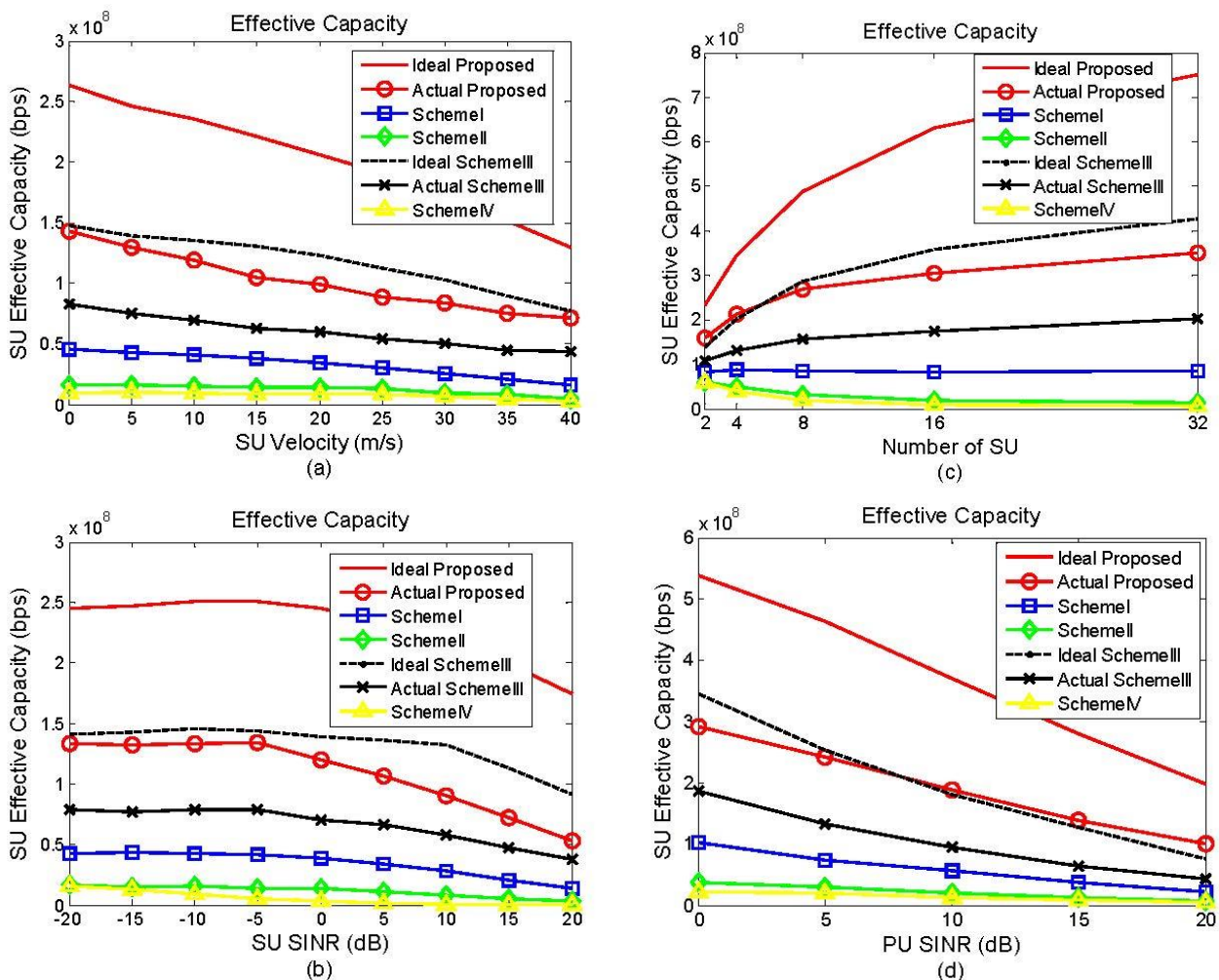


Figure 3. Total Average Effective Capacity versus SUs' SINR requirements for different schemes.

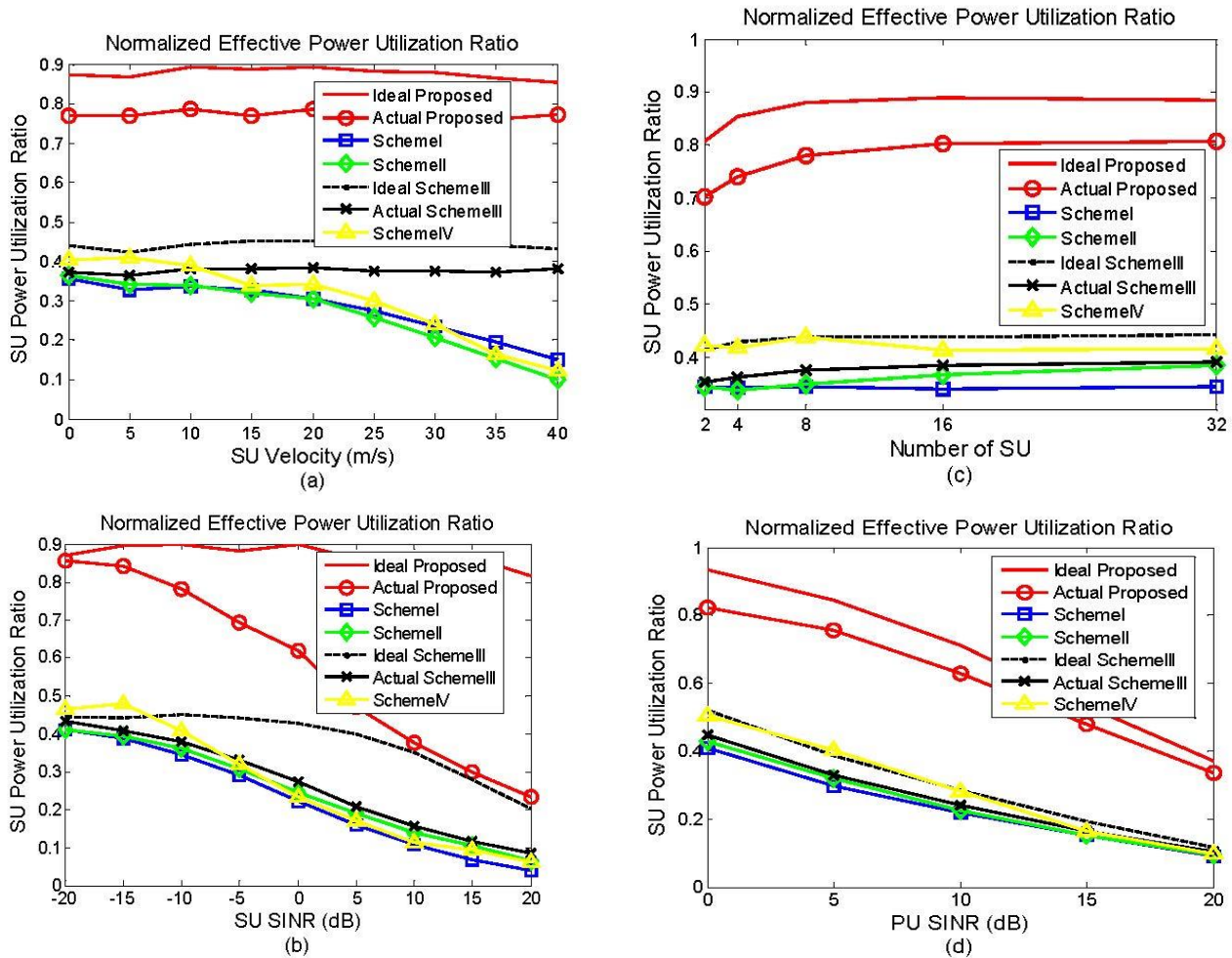


Figure 4. Power Utilization Ratio versus PUs' SINR requirements for different Schemes.

significantly by means of the proposed power enhancement. From Fig. 4(b), the secondary power utilization ratio of the Idea Proposed Scheme remains stable, whereas that for the Actual Proposed Scheme drops quickly. This difference occurs because when the secondary SINR target is higher, the prediction error brought about by the location-correlated shadow fading will have more significant influence on the proposed power allocation and the secondary EE.

In Fig. 4(c), as the number of SUs is varied, the secondary power utilization ratio is found to increase slightly and then quickly remain stable. As shown in Fig. 4(d), the primary minimum SINR demands have a similar effect on the secondary power utilization ratio, compared to Fig. 3(d). As a result, our RA scheme also improves the secondary EE according to the admission control proposed and the enhanced water-filling strategy, avoiding wasting power on the subchannels with poor conditions or to the SUs moving beyond the cell.

In Fig. 5, we plot the performance curves in terms of the secondary subchannel utilization ratio for the different schemes. We define the subchannel utilization ratio as the

ratio of the effectively assigned subchannels' number to that of the subchannels fully provided. Thus, the secondary SE performance for the simulated schemes can be evaluated. The secondary subchannel utilization ratio for the proposed scheme is robust as the secondary speed increases according to the comparison shown in Fig. 5(a). It is attributed to the anti-shadowing CSI predicting and the enhanced power allocation method.

According to Fig. 5(b), the performances for all schemes decline with the secondary SINR target growing, including the ideal schemes. It is reasonable that the water-filling based power allocation method is able to utilize the secondary power budget adequately, whereas the proposed access control and subchannel assignment scheme based on the anti-shadowing CSI prediction cannot be similarly considered. For the simulation results in Fig. 5(c) and Fig. 5(d), the performances plotted are similar to those in Fig. 4.

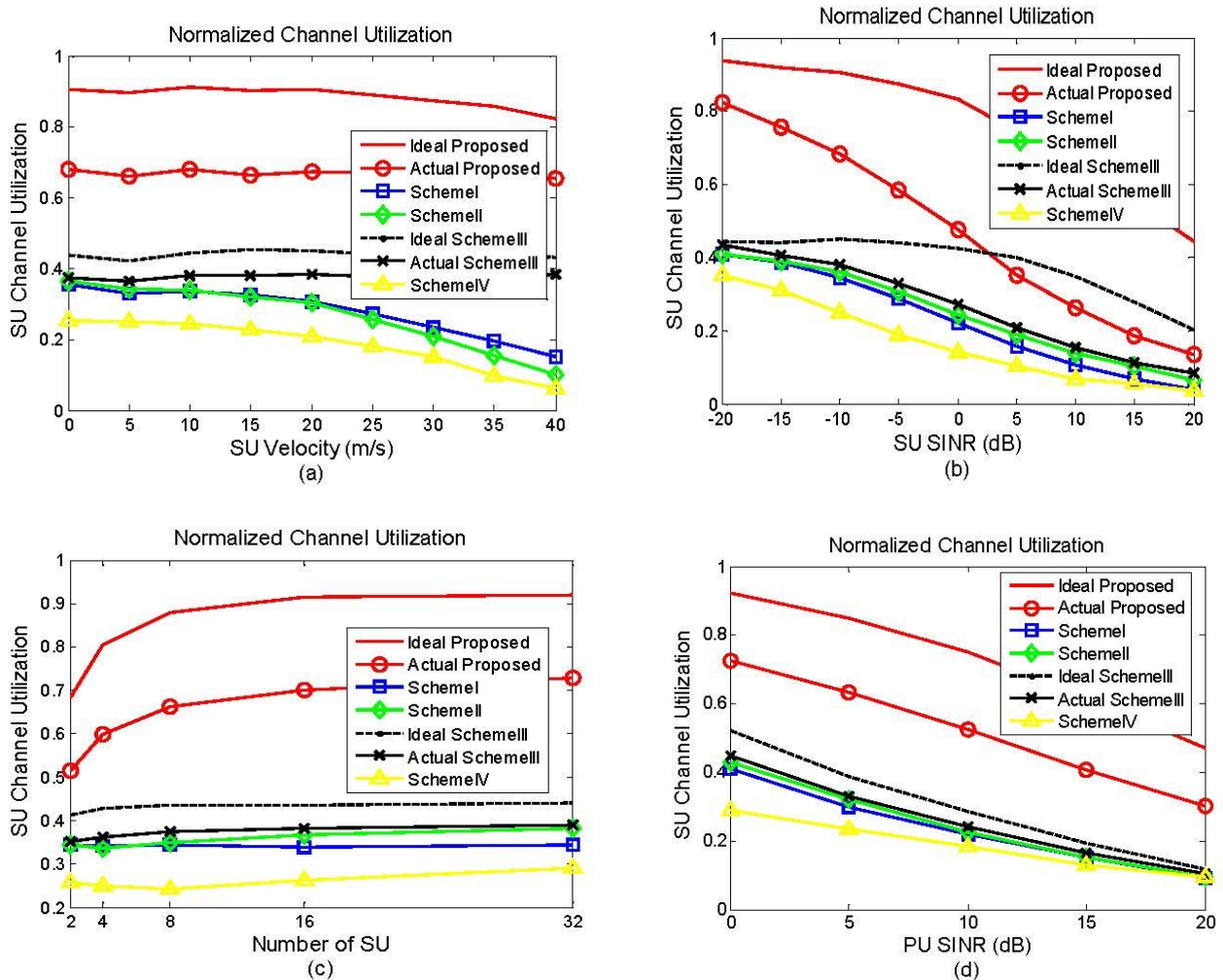


Figure 5. Subchannel Utilization Ratio versus PUs' SINR requirements for different schemes.

Therefore, similar conclusions can be obtained based on the abovementioned analytical results.

VII. Conclusion

In this paper, we presented an anti-shadowing subchannel and power resource allocation method for OFDMA-based mobile SUs in cellular CRNs, aiming at maximization of the total secondary effective capacity. Considering the diversity of locations and channel conditions for the mobile SUs, an anti-shadowing CSI prediction method was proposed. A stepwise resource allocation algorithm with low complexity was introduced to make the problem tractable. Using this original algorithm, extension schemes could be deduced similarly for the general mobile CRNs with moving PUs. Compared with some previous schemes, the simulation results revealed the relationships between the secondary performances and various system parameters. Moreover, the benefits of our original scheme were verified in terms of the effective capacity, energy efficiency and spectrum efficiency.

Reference

- [1] Guoru Ding, Jinlong Wang, Qihui Wu, Yu-dong Yao, Rongpeng Li, Honggang Zhang, Yulong Zou, "On the limits of predictability in real-world radio spectrum state dynamics: from entropy theory to 5G spectrum sharing," *IEEE Communications Magazine*, vol. 53, no. 7, 2015.
- [2] H. Mahmoud, T. Yucek and H. Arslan, "OFDM for cognitive radio: merits and challenges," *IEEE Wireless Communications*, vol. 16, no. 2, pp. 6-15, 2009.
- [3] I. F. Akyildiz, W.Y. Lee, M. C. Vuran and S. Mohanty, "Next generation dynamic spectrum access cognitive radio wireless networks: A survey," *Computer Networks (Elsevier)*, vol. 50, pp. 2127-2159, 2006.
- [4] S. Srinivasa and S. A. Jafar, "Cognitive radio for dynamic spectrum access-The throughput potential of cognitive radio: A theoretical perspective," *IEEE Communication Magazine*, vol. 45, pp. 73-79, 2007.
- [5] Y. Song and J. Xie, "Optimal power control for concurrent transmissions of location-aware mobile cognitive radio ad hoc networks," *IEEE GLOBECOM*, pp. 1-6, 2009.
- [6] A. W. Min, K.H. Kim, J. P. Singh and K. G. Shin, "Opportunistic spectrum access for mobile cognitive radios," *IEEE INFOCOM*, pp. 2993-3001, 2011.9
- [7] S. Jana, K. Zeng, W. Cheng and P. Mohapatra, "Trusted collaborative spectrum sensing for mobile cognitive radio networks," *IEEE Transactions on Information Forensics and Security*, vol. 8, pp. 2621-2625, 2013.

- [8] G. Han, J. Jiang, C. Zhang, T. Q. Duong, M. Guizani and G. Karagiannidis, "A Survey on Mobile Anchors Assisted Localization in Wireless Sensor Networks," *IEEE Communications Surveys & Tutorials*, vol. 18, No. 3, pp. 2220-2243, 2016.
- [9] G. Han, X. Yang, L. Liu, W. Zhang and M. Guizani, "A Disaster Management-Oriented Path Planning for Mobile Anchor-Based Localization in Wireless Sensor Networks," *IEEE Transactions on Emerging Topics in Computing*, 2017, DOI: 10.1109/TETC.2017.2687319.
- [10] G. Han, L. Liu, S. Chan, R. Yu and Y. Yang, "HySense: A Hybrid Mobile CrowdSensing Framework for Sensing Opportunities Compensation under Dynamic Coverage Constraint," *IEEE Communications Magazine*, vol. 55, No. 3, pp. 93-99, 2017
- [11] Y. Lu and A. D. Hallen, "Channel-aware spectrum sensing and access for mobile cognitive radio ad hoc networks," *IEEE Transactions on Vehicular Technology*, vol. 65, no. 4, pp. 2471-2480, 2016.
- [12] Y. Chen, S. Zhang, S. Xu and G. Li, "Fundamental tradeoffs on green wireless networks," *IEEE Communication Magazine*, vol. 49, no. 6, pp. 30-37, 2011.
- [13] N. Forouzan and S. A. Ghorashi, "New algorithm for joint sub-channel and power allocation in multi-cell OFDMA-based cognitive radio networks," *IET Communications*, vol. 8, pp. 508-515, 2014.
- [14] A. S. Cacciapuoti, M. Caleffi, L. Paura and M. A. Rahman, "Channel availability for mobile cognitive radio networks," *Journal of Network and Computer Applications*, vol. 47, pp. 131-136, 2015.
- [15] H. W. Kuhn, "The Hungarian method for the assignment problem," *Naval Research Logistics*, vol. 52, no. 1, pp. 7-21, 2005.
- [16] K. Yang, N. Prasad and X. Wang "A message-passing approach to distributed resource allocation in uplink DFT-spread-OFDMA systems," *IEEE Transactions on Communications*, vol. 59, pp. 1099-1113, 2011.
- [17] Shaowei Wang and Chen Ran, "Rethinking cellular network planning and optimization," *IEEE Wireless Communications*, vol. 23, no. 2, pp. 118-125, 2016.
- [18] Chenhao Qi, Lenan Wu, Yongming Huang and A. Nallanathan, "Joint Design of Pilot Power and Pilot Pattern for Sparse Cognitive Radio Systems," *IEEE Transactions on Vehicular Technology*, vol. 64, no. 11, pp. 5384 – 5390, 2015.